Excitation and ionization cross sections for fast lithium atoms and ions colliding with atoms

George H. Gillespie
Physical Dynamics, Inc., P.O. Box 1883, La Jolla, California 92038
(Received 2 July 1982)

The results of a comprehensive study of projectile excitation and ionization cross sections for fast lithium atoms and positive ions impacting on low-Z (≤ 11) targets are presented. This theoretical study is based on an asymptotic (high-speed) form of the Born approximation and the emphasis is placed on establishing the principal collision processes for Li^0 at high energies, including inner-shell and valence-shell transitions to both discrete and continuum final states. An extensive comparison with experimental results for H_2, He, and N targets is included. Recent experimental data for the Li^0 $2P$-$2S$ emission cross sections for He targets in the 10—100-keV/u energy regime are in good agreement with the theoretical results, although significant departures from the trend of those data are predicted for higher energies due to the onset of doubly inelastic processes. Some discrepancies with recently reported Li^0 electron-loss cross sections at $\frac{6}{7}$ MeV/u are noted for several targets.

I. INTRODUCTION

There has recently been increased interest in the use of fast, light ($A \lesssim 20$ u) ion and atom beams for a variety of applications. Ion beam lithography,[1] light-ion inertial fusion,[2] and neutral-beam plasma heating[3] are some of the areas currently under active research and development. Since several of these applications envisage using ions only partially stripped, or even neutral atoms, collision processes involving excitation and ionization of such projectiles are frequently of interest. This paper reports the results of a case study of Born-approximation calculations for such cross sections for fast lithium atoms and ions colliding with neutral atoms. In addition to its possible applications, lithium is of particular theoretical interest in this regard from both the basic atomic physics standpoint as the simplest ground-state multishell atom and because of several recent experimental studies[4–6] examining the production of neutral lithium atoms using collisional electron detachment from Li^- in the MeV energy regime.

The calculations reported in this paper are based on an asymptotic (high-energy) expansion of the Born approximation. The details of this type of calculation have been described in previous papers,[7] and the results essential for this work may be summarized in a few lines. The cross sections of interest in this work have an asymptotic velocity (v) dependence of the form

$$\sigma = 8\pi a_0^2 \frac{\alpha^2}{\beta^2}\left[I + \frac{\alpha^2}{\beta^2}\gamma\right],$$
$$= 3.75\times 10^{-20}\left[I + \frac{\alpha^2}{\beta}\gamma\right]\Big/\beta^2, \quad (1)$$

where σ is expressed in units of cm^2, and where $\beta = v/c$, α is the fine-structure constant, and a_0 is the Bohr radius. The term in parentheses,

$$I + \frac{\alpha^2}{\beta^2}\gamma,$$

is the collision strength to two orders in this v^{-2} expansion. The coefficient I may be calculated as a (numerical) integral over momentum transfer K, of the product of two transition strengths, one each describing the projectile atom or ion $S(K)$, and the target atom $\mathcal{F}(K)$:

$$I = \int_0^\infty S(K)\mathcal{F}(K)\frac{d(a_0K)}{(a_0K)^3}. \quad (2)$$

The second-order collision strength γ, may be computed (approximately) from the dipole oscillator strengths of the projectile and target.[7]

The target-atom transition strengths $\mathcal{F}(K)$ appearing in Eq. (2) are divided into only two classes in order to facilitate the numerical computations, those in which the final state is the same as the initial state, and those for which the target atom is in any other possible state. Following previous notations, the collision strengths for a particular process are labeled by an ordered pair of subscripts, with

the second subscript referring to these two classes of target final states, el (for elastic) or in (for inelastic), respectively. The first subscript is reserved for labeling the particular transition of the incident projectile. For example, the total collision strength for the ionization of a projectile lithium atom colliding with a neutral target atom consists of two contributions $I_{\text{ion,el}}$ and $I_{\text{ion,in}}$ with

$$I_{\text{ion,el}} = \int_0^\infty S_{\text{ion}}(K)\mathcal{F}_{\text{el}}(K)\frac{d(a_0K)}{(a_0K)^3} , \tag{3}$$

$$I_{\text{ion,in}} = \int_0^\infty S_{\text{ion}}(K)\mathcal{F}_{\text{in}}(K)\frac{d(a_0K)}{(a_0K)^3} . \tag{4}$$

The factors $\mathcal{F}_{\text{el(in)}}(K)$ correspond, respectively, to the square of the target elastic form factor and the target incoherent scattering function, both of which may be obtained from tabulated data such as those given by Hubbell *et al.*[8] The function $S_{\text{ion}}(K)$ is the total ionization transition strength for neutral lithium, which is discussed in detail in the following section.

II. TRANSITION STRENGTHS FOR LITHIUM ATOMS AND IONS

A. Neutral lithium

The transition strengths for discrete final states may be readily computed if the generalized oscillator strengths $f(K)$ for the transition are available, viz,

$$S_{2S\to NL}(K) = \frac{(a_0K)^2}{E_{2S\to NL}} f_{2S\to NL}(K) , \tag{5}$$

for excitations from the valence shell of Li. Here, $E_{2S\to NL}$ is the energy difference between the $2S$ and NL states, in rydbergs. For final states in the continuum, a numerical integral over final-state energies must be performed. If $df_{2S\to C}(K,E)/dE$ denotes the generalized oscillator strength for transitions from the valence shell to all continuum final states of excitation energy E, then the corresponding transition strength is

$$S_{2S\to C}(K) = (a_0K)^2 \int_{E_B}^\infty \frac{df_{2S\to C}(K,E)}{dE}\frac{dE}{E} , \tag{6}$$

where E_B is the threshold energy (ionization potential) in rydbergs. [Note that Eqs. (2)–(6) implicitly assume that final magnetic substates have been summed over, so that results depend only on the magnitude K of momentum transfer.]

For atomic lithium, transition strengths have been computed for both valence- and inner-shell transitions from the generalized-oscillator-strength data of McGuire.[9] These oscillator strengths are for transitions involving one electron moving in the Herman-Skillman (HS) model central potential.[10] For the case of discrete final states of the valence shell, calculations have also been carried out from the Hartree-Fock (HF) generalized oscillator strengths computed by Kim and Cheng.[11] Figure 1 summarizes the results for the principle transition strengths of neutral Li.

Several important features of the transition strengths for atomic lithium are apparent from Fig. 1. For the valence-shell transitions leading to discrete final states [Figs. 1(a) and 1(b)], the HF and HS transition strengths shown are in generally good agreement (within 10%) over the region of momentum transfer encompassing the maxima. There are zeros in these transition strengths for $a_0K > 1$, and in the case of NP ($N \geq 3$) final states [Fig. 1(a)] also for $a_0K < 0.3$. These are not apparent in the figures since the transition strengths become negligibly small on the scale of the figures for regions of momentum transfer beyond the zeros. As might be expected, the HF and HS transition strengths frequently differ significantly near the zeros, but the magnitudes themselves are so small that no differences of substance can be anticipated when evaluating collision strength integrals via Eq. (2).

The (low-K) zeros in the $2S\to NP$ ($N \geq 3$) lithium transition strengths, and the general smallest of the transition strengths for a_0K values below that point, yield a sizable region of low momentum transfer in which nondipole allowed transitions are important. This is clear from Fig. 1(a) where the final S and D states dominate the corresponding (same principal quantum number) P-state transition strengths for essentially all values of momentum transfer in the figure below its peak value. Of course at very small values of a_0K the P-state transition strengths eventually dominate; for $2S\to NL$ with $N \geq 3$ this region corresponds to $a_0K < 10^{-1}$. The $2S\to 2P$ transition strength is itself larger than all the remaining discrete-state transition strengths taken together for $a_0K \lesssim 0.8$. This is clearly displayed in Fig. 1(b); note also the order-of-magnitude change in vertical scale from Fig. 1(a). Thus, when all taken together, one dipole-allowed transition ($2S\to 2P$) dominates excitations in the entire low-momentum-transfer region.

For the inner-shell transition strengths ($1S\to NL$

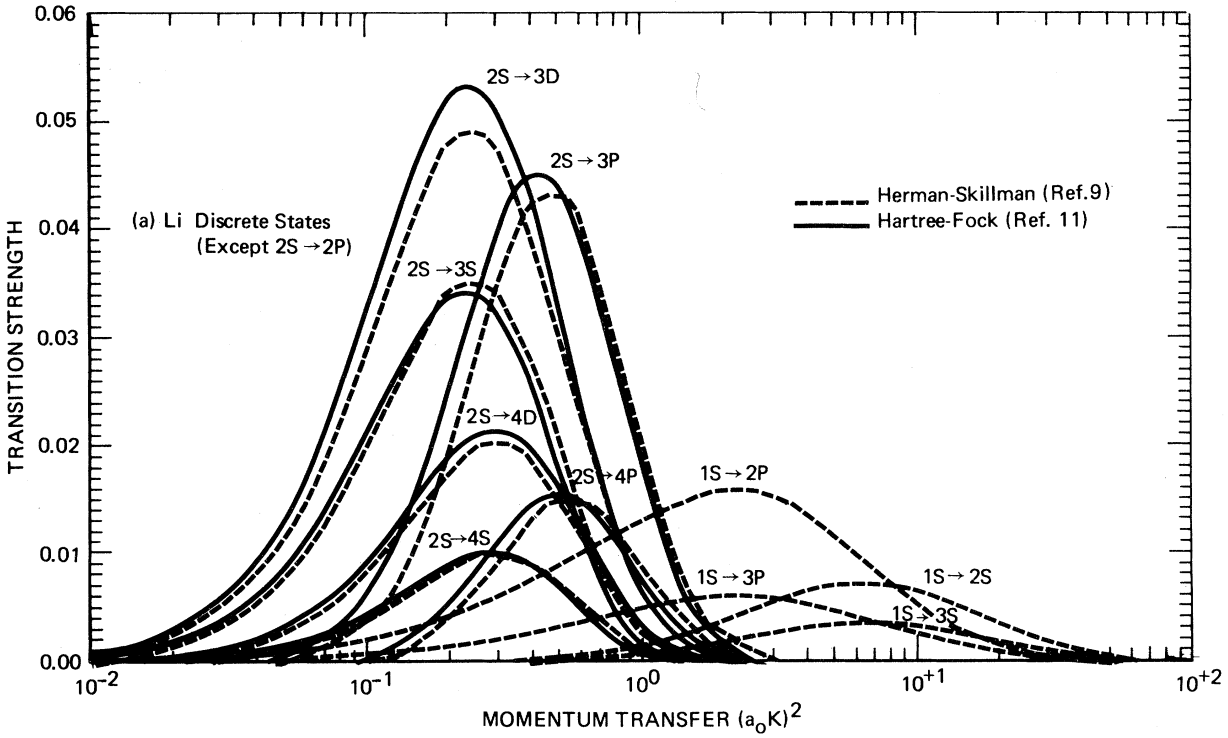

FIG. 1. Transition strengths as a function of momentum transfer for atomic lithium for (a) select discrete final states, except for the dominant $2S \rightarrow 2P$ transition, (b) the $2S \rightarrow 2P$ transition and sums over discrete final states, and (c) total discrete-final-state and continuum-final-state transition strengths. In (a) and (b) the valence-shell transitions ($2S \rightarrow NL$) given by solid curves are based on the Hartree-Fock generalized oscillator strengths of Kim and Cheng (Ref. 11) computed according to Eq. (5). For both the valence-shell and inner-shell transitions ($1S \rightarrow NL$) the dashed curves are based on the Herman-Skillman generalized oscillator strengths computed by McGuire (Refs. 9 and 12). Total (discrete) excitation transition strengths shown in (b) and (c) also include contributions from higher N states than given in (a). Total ionization transition strengths ($2S \rightarrow C$ and $1S \rightarrow C$) are computed according to Eq. (6) from McGuire's continuum generalized oscillator strengths (Ref. 9). Also included in (c) are Li incoherent scattering functions computed in Hartree-Fock (Ref. 11, solid curve) and configuration-interaction models (Ref. 8, dashed curve), which provide independent checks on the sum of all the transition strengths ($S_{1S,2S\rightarrow\Sigma}$, dotted curve).

transitions in Fig. 1), the generalized oscillator strengths of McGuire[9] have again been used. These are clearly much smaller than the valence-shell transition strengths and peak at a significantly higher momentum transfer, reflecting the much larger energy difference between inital and final states. These are qualitatively similar to the hydrogenic transition strengths discussed in previous work.[7] As in that case, the NP final states dominate and the NS final states are of secondary importance. The transition strengths $1S \rightarrow ND$ are quite small and would be imperceptible on the scale used in Fig. 1(c). This is in marked contrast to the importance of ND and NS states for valence-shell transitions to the same principal quantum number final states. It should also be noted that the decay of these, the inner-shell excitations for Li^0, will be strongly dominated by Auger electron emission rather than by photon emission; i.e., these final states will be primarily autoionizing states.

The transition strengths for continuum final states which result in ionization from both the valence shell and the inner shell have been calculated [Eq. (6)] from the corresponding generalized-oscillator-strength data of McGuire. For sufficiently large momentum transfer, these transition strengths approach asymptotic limits which are equal to the number of electrons in the initial shell. At such large momentum transfer, the integral over the energy of the final state [Eq. (6)] is dominated by the region near $E=(a_0K)^2$, i.e., the Bethe ridge in the generalized-oscillator-strength surface. This ridge is not always well represented by the values of E and K at which McGuire's calculations are tabulated and there is some uncertainty in extrapolations in those regions. For the transition strengths shown

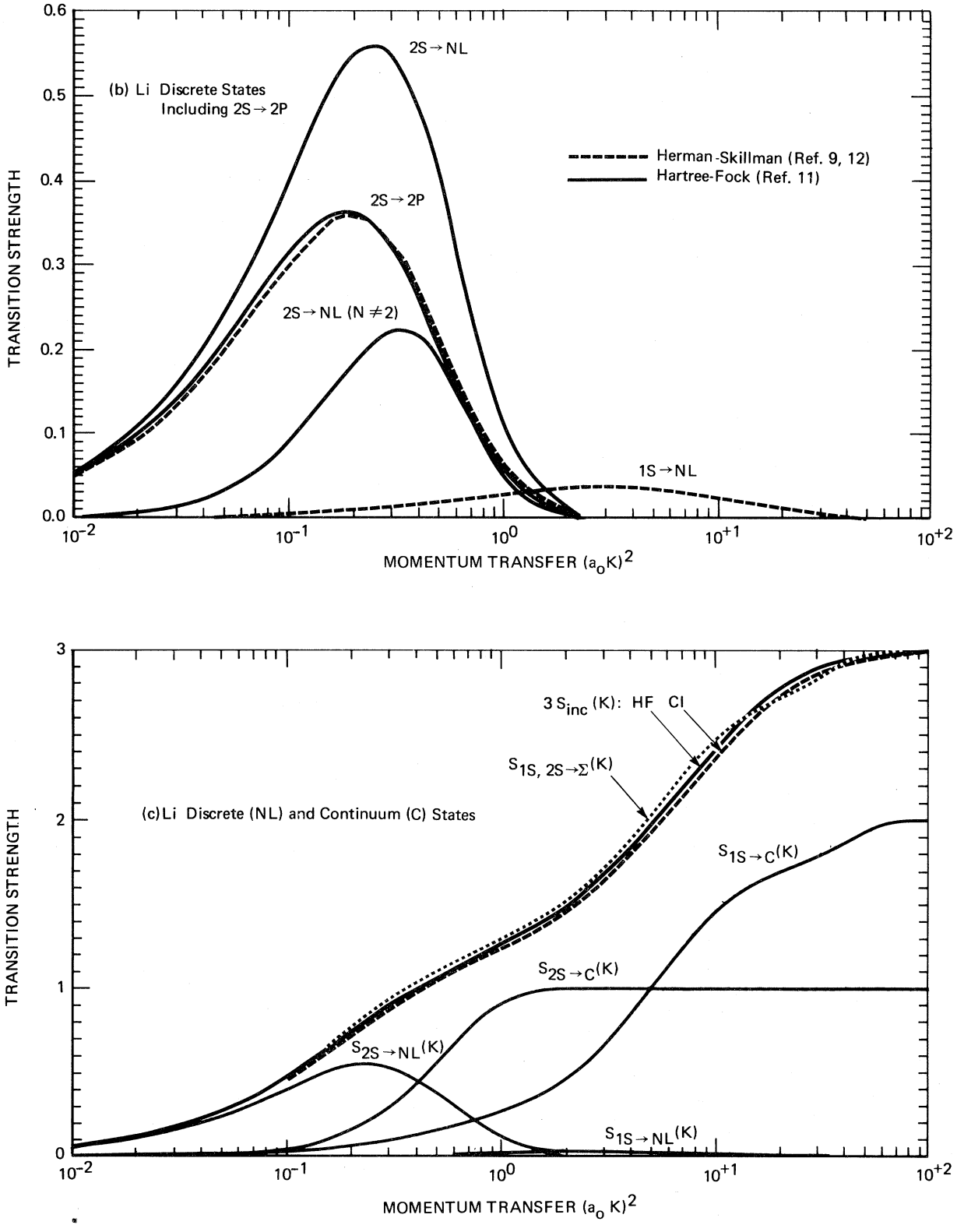

FIG. 1. (*Continued.*)

in Fig. 1(c), the asymptotic value was fixed for all K values greater than that for which the asymptote was first attained via numerical integration. [Typically, values of $S_{2S\to C}(K)$ computed numerically for $(a_0K)^2 \geq 2$, and of $S_{1S\to C}(K)$ for $(a_0K)^2 \geq 70$, were within 10–20% or so of the asymptotic value, reflecting this uncertainty.]

The total ionization collision strength S_{ion} for Li^0 will be given by

$$S_{\text{ion}}(K)=S_{1S\to C}(K)+S_{2S\to C}(K) + S_{1S\to NL}(K) , \quad (7)$$

where the last term assumes that all inner-shell excitations lead to autoionization. It is clear from Fig. 1(c), however, that it is quite small compared to the first two terms in Eq. (7), and that for most applications, the total ionization collision strengths given by Eqs. (3) and (4) may be calculated to within a few percent by including only $S_{1S\to C}(K)$ and $S_{2S\to C}(K)$. Note also that whereas $S_{2S\to C}(K)$ leads to Li^+ in the $(1S^2)^1S$ final state, $S_{1S\to C}(K)$ leads to $(1S2S)^1S$ and ^3S Li^+ final states in the context of the Herman-Skillman model.

As an overall check on the transition strengths, Fig. 1(c) also displays the incoherent scattering function of Li, computed both in Hartree-Fock approximation (solid curve) and for a wave function which includes configuration interactions (CI, dashed curve).[8] The sum rule

$$S_{1S,2S\to\Sigma}(K)=3S_{\text{inc}}(K) , \quad (8)$$

where $S_{1S,2S\to\Sigma}(K)$ is the sum of all the transition strengths computed, provides a powerful overall check on the self-consistency of the transition strengths. This sum is given by the dotted curve and it is clear that there are no major discrepancies with Eq. (8). This sum is within 5% of the HF incoherent scattering function, generally being slightly above. Near $(a_0K)^2=30$, the sum is below the value of $3S_{\text{inc}}(K)$ for either model of the ground state. This dip is due to the slight undulation in the computed inner-shell ionization transition strength $S_{1S\to C}(K)$ and is a reflection of the limited accuracy in evaluating the integral over final-state energy. (This region of K contributes very little to the collision strength integrals [Eq. (2)] and small improvements in the transition strength here would not affect any results for those.)

In addition to the transition strengths displayed in Fig. 1, various energy moments of the dipole-oscillator strengths for neutral lithium have been computed. These are required for evaluating the second-order collision strengths [γ in Eq. (1)] and also provide a further check on the self-consistency of the oscillator strength data used in Eqs. (5) and (6). Table I summarizes the results for selected energy moments obtained from McGuire's data.[9,12] For comparison, Table I also includes other results from the literature for Li^0, Li^+, and Li^{2+}. The differences (never greater than 5.6%) between the partial and total moments obtained from McGuire's

TABLE I. Partial and total μth-energy moments of the dipole-oscillator-strength distribution $\sum(\epsilon_n)^\mu f_n$ for Li^0, Li^+, and Li^{2+}. The results computed in this work for neutral Li are based on the oscillator-strength data of McGuire (Ref. 9). In addition, select results for Li from Ref. 15, also computed from a Herman-Skillman model, are given. In no case has a difference of more than about $5\frac{1}{2}$% been found for any total or partial Li^0 energy moment. (See, however, Ref. 15 for values obtained using other atomic models and/or experimental data.)

Atomic system	Moment μ	Discrete K-shell contribution	Discrete L-shell contribution	Continuum K-shell contribution	Continuum L-shell contribution	Total moment
Li^0	−1	0.0403	5.405	0.255	0.224	5.924
			5.3703[a]		0.2114[a]	5.865[a]
	0	0.172	0.772	1.938	0.238	3.120
			0.7755[a]		0.2244[a]	3.000[a]
	+1	0.735	0.112	20.4	0.558	21.8
						21.0[a]
Li^+[b]	−1	0.1415		0.1445		0.2860
	0	0.676		1.324		2.000
	+1	3.24		16.94		20.18
Li^{2+}[c]	−1	0.079 62		0.031 49		$\frac{1}{9}$
	0	0.5650		0.4350		1
	+1	4.044		7.956		12

[a]Herman-Skillman model, Ref. 15.
[b]All Li^+ values from Ref. 13.
[c]All Li^{2+} values from Ref. 7.

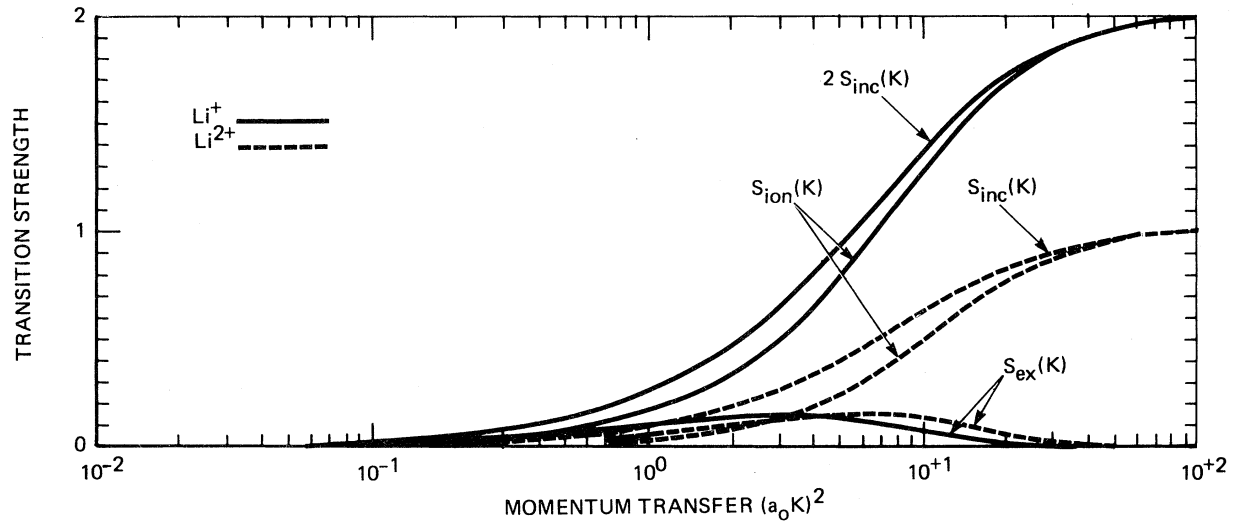

FIG. 2. Transition strengths for Li^+ and Li^{2+} as a function of momentum transfer. Shown for each ion are the total excitation transition strength $S_{ex}(K)$ and the total ionization transition strength $S_{ion}(K)$, as well as their sum given by the incoherent scattering functions $S_{inc}(K)$. For Li^+, the excitation transition strength is based on generalized oscillator strengths computed from accurate Weiss wave functions by Kim (Ref. 13); the incoherent scattering function is also due to Kim (Ref. 14) for the corresponding Weiss ground-state wave function. Li^+ ionization transition strength has been computed from the difference $2S_{inc}(K)-S_{ex}(K)$. For the hydrogenic ion Li^{2+}, the transition strengths are from Ref. 7.

data and those reported in Ref. 15 for the Herman-Skillman model reaffirm that there are no major inconsistencies in the low-K transition strengths for neutral lithium.

B. Positive lithium ions

For the hydrogenic ion Li^{2+} the transition strengths may be obtained directly from results given in Ref. 7. For the heliumlike ion Li^+ the discrete final-state transition strengths have been computed from the generalized-oscillator-strength data described by Kim and Inokuti.[13] Together with the incoherent scattering functions for these ions,[7,14] the total transition strengths for discrete final states $[S_{ex}(K)]$ and continuum final states $[S_{ion}(K)]$ are summarized in Fig. 2. In the case of Li^+, the ionization transition strength shown is the apparent value of $S_{ion}(K)=2S_{inc}(K)-S_{ex}(K)$, where $S_{ex}(K)$ has been calculated by summing the individual contributions of each discrete state (including an N^{-3} extrapolation for highly excited final states).

Only a few comments on the relative magnitudes of the various transition strengths for these ions will be included here, since the features of Li^+ and Li^{2+} are generally similar and this later hydrogenic case has been discussed in detail previously.[7] First, as would be expected, there are obvious similarities between the Li^+ transition strengths, $S_{ion}(K)$ and $S_{ex}(K)$, and the Li^0 K-shell transition strengths, $S_{1S\to C}(K)$ and $S_{1S\to NL}(K)$. There is, however, a more precise relationship among these for all of the Li charge states. Physically, since the $2S$ electron in Li^0 offers some screening in both the initial and final states as compared to Li^+, one anticipates that K-shell ionization from Li^0 should be more likely than it is for Li^+. Similarly, since one of the K-shell electrons in Li^+ offers some screening for the other, one can expect that Li^+ ionization should be more than twice as probable as Li^{2+} ionization. Specifically then, the following relationship is anticipated:

$$S_{1S\to C}^{Li^0}(K)\geq S_{ion}^{Li^+}(K)\geq 2S_{ion}^{Li^{2+}}(K)\ . \tag{9}$$

This relationship is verified by the numerical computations of this work, with the exception of the region near $(a_0K)^2=30$ where, as noted earlier, the calculated values of $S_{1S\to C}(K)$ for Li^0 are too low due to the limited data available for the corresponding generalized oscillator strength in that momentum-transfer region. If in fact one corrects the values of $S_{1S\to C}(K)$ by the amount "missing" as determined by the sum rule $[3S_{inc}(K)-S_{1S,2S\to\Sigma}(K)$ from Fig. 1(c)] in this region, then the first inequality in Eq. (9) is also satisfied near $(a_0K)^2=30$.

As a further comment on the ordering of the transition strengths given by (9), it is noted that the equality in each case is only attained as $K\to\infty$, and that the maximum inequality is attained in the $K\to 0$ limit. This latter limit results in very rough-

ly a factor of 2 difference in the transition strengths, as can be seen from the contributions to the $\mu=-1$ energy moments of dipole-oscillator-strength distribution arising from the K-shell transitions to the continuum given in Table I.

For the case of discrete excitations, the ordering is reversed:

$$S^{\mathrm{Li}^0}_{1S\to NL}(K)<S^{\mathrm{Li}^+}_{\mathrm{ex}}(K)<2S^{\mathrm{Li}^{2+}}_{\mathrm{ex}}(K)\ . \tag{10}$$

In essence, this is because the active electron in each case sees an increasingly stronger effective potential, and transitions among the bound states become relatively easier than transitions to the continuum. This type of inequality (for discrete states) is less general in nature than that for continuum final states, Eq. (9). For example, the discrete-state valence-shell transition strength $S_{2S\to NL}(K)$ for neutral lithium is less than $S_{\mathrm{ex}}(K)$ for a $2S$ hydrogenlike projectile[16] only if the atomic number is adjusted to an effective value of about 1.4, whereas the relation analogous to Eq. (9) for valence-shell ionization is still satisified, i.e.,

$$S^{\mathrm{Li}^0}_{2S\to C}(K)\geq S^{\mathrm{Li}^{2+}(2S)}_{\mathrm{ion}}(K)\ . \tag{11}$$

This inequality is also satisifed as long as the effective atomic number of the $2S$ hydrogenlike ion is greater than about 2.

As a matter of practical interest, it should be noted that the K-shell and L-shell contributions to the incoherent scattering factor can be very closely approximated (*a few percent for all K)* by the corresponding hydrogenic functions

$$S^{1S}_{\mathrm{inc}}(K)=N_{1S}-N_{1S}[1+(a_0K/2Z^*)^2]^{-4}\ , \tag{12}$$

$$S^{2S}_{\mathrm{inc}}(K)=N_{2S}-N_{2S}\{[1-(a_0K/Z^*)^2][1-2(a_0K/Z^*)^2]/[1+(a_0K/Z^*)^2]^4\}^2\ . \tag{13}$$

The number of electrons in each shell is given by N_{1S} or N_{2S} ($=1$ or 2), and the effective Z^* values are 3 for $\mathrm{Li}^{2+}(1S)$, 2.72 for $\mathrm{Li}^+(1S)$, 2.57 for $\mathrm{Li}^0(1S)$, and 1.58 for $\mathrm{Li}^0(2S)$. As is apparent from the discussion, such simple scalings for the discrete and continuum final states separately are not nearly as accurate.

III. ASYMPTOTIC COLLISION STRENGTHS

The transition strengths discussed in the preceding section have been utilized to compute asymptotic collision strengths via Eq. (2) for several low-Z target atoms and molecular H_2. The only target properties required for these computations are the atomic form factor $F(K)$, and the incoherent scattering function $S_{\mathrm{inc}}(K)$, i.e., substituting

$$\mathscr{F}_{\mathrm{el}}(K)=|\,Z-F(K)\,|^2 \tag{14}$$

and

$$\mathscr{F}_{\mathrm{in}}(K)=ZS_{\mathrm{inc}}(K) \tag{15}$$

into Eqs. (3) and (4), for example. The calculations carried out for this work have utilized the tabulations of Hubbell *et al.*[8] for $F(K)$ and $S_{\mathrm{inc}}(K)$ for neutral atoms, and those of Liu and Smith[17] for molecular H_2. For atomic nitrogen targets, some calculations have also been performed using configuration-interaction wave-function results for $F(K)$ and $S_{\mathrm{inc}}(K)$ given by Tanaka and Sasaki[18]; this permits a comparison with the computations based on Hubbell's data which is for a Hartree-Fock nitrogen wave function.

A comprehensive set of calculations have been completed for H_2, He, and N targets; only select (primarily ionization) collision strengths have been computed for other ($Z\leq 11$) targets. Neutral lithium projectiles offer the richest variety of inelastic processes and the emphasis in this work is on those collision strengths. A fairly complete set of results is given for Li^0 then, with only some representative results included for Li^+ and Li^{2+}.

A. Discrete final states

Table II gives a summary of the collision strengths computed for the discrete transitions of Li^0 in collisions with He, H_2, and N. The results presented include excitations from the (a) K shell and (b) L shell, using the transition strengths computed from McGuire's data,[9,12] as well as (c) valence-shell transitions calculated from the data of Kim and Cheng.[11] In each case, results are given for the first few S, P, and D final states ($N<5$), and an approximate extrapolation formula useful for estimating collision strengths for higher-N final states is included. These results are then used to obtain total inner-shell and valence-shell excitation collision strengths. For the Hartree-Fock case in Table II(c), collision strengths for NP final states up to $N=7$ are included in order to display, by way of ex-

TABLE II. Collision strengths for discrete final states of neutral lithium in high-speed collisions with He, H_2, and N: (a) Collision strengths for the inner-shell excitation of Li^0 using Herman-Skillman transition strengths. These results are based on the Li^0 generalized oscillator strengths of McGuire (Ref. 9), and on the atomic form factors and incoherent scattering functions of Hubbell, *et al.* (Ref. 8) for He, Liu and Smith (Ref. 17) for H_2, and Tanaka and Sasaki (Ref. 18) for N. (b) Collision strengths for the valence-shell excitation of Li^0 using Herman-Skillman transition strengths. These results are based on the Li^0 generalized oscillator strengths of McGuire (Refs. 9 and 12), and on the atomic form factors and incoherent scattering functions of Hubbell *et al.* (Ref. 8) for He and N, and Liu and Smith (Ref. 17) for H_2. (c) Collision strengths for the valence-shell excitation of Li^0 using Hartree-Fock strengths. These results are based on the Li^0 generalized oscillator strengths of Kim and Cheng (Ref. 11), and on the atomic form factors and incoherent scattering functions of Hubbell *et al.* (Ref. 8) for He and N, and Liu and Smith (Ref. 17) for H_2. The first subscript (NL) on the collision strengths ($I_{NL,el}$ and $I_{NL,in}$) refers to the Li^0 final state, the second (el or in) refers to whether the target is scattered elastically or inelastically. Also included are total inelastic collision strengths computed from Hartree-Fock and configuration interaction Li^0 ground-state wave functions.

Li Final State (NL)	He $I_{NL,el}$	He $I_{NL,in}$	H_2 $I_{NL,el}$	H_2 $I_{NL,in}$	N $I_{NL,el}$	N $I_{NL,in}$
			(a) Inner-shell excitation of Li^0			
$1S \rightarrow 2P$	3.54×10^{-3}	1.23×10^{-2}	5.01×10^{-3}	2.04×10^{-2}	6.26×10^{-2}	3.71×10^{-2}
$3P$	1.41×10^{-3}	4.55×10^{-3}	1.93×10^{-3}	7.48×10^{-3}	2.45×10^{-2}	1.37×10^{-2}
$4P$	5.83×10^{-4}	1.87×10^{-3}	7.94×10^{-4}	3.07×10^{-3}	1.01×10^{-2}	5.63×10^{-3}
NP ($N\geq5$)	$0.037N^{-3}$	$0.12N^{-3}$	$0.051N^{-3}$	$0.20N^{-3}$	$0.65N^{-3}$	$0.36N^{-3}$
All NP	0.006 44	0.0216	0.008 97	0.0358	0.113	0.0652
$1S \rightarrow 2S$	1.66×10^{-3}	2.57×10^{-3}	1.60×10^{-3}	3.58×10^{-3}	2.41×10^{-2}	7.37×10^{-3}
$3S$	7.60×10^{-4}	1.13×10^{-3}	7.11×10^{-4}	1.55×10^{-3}	1.09×10^{-2}	3.23×10^{-3}
$4S$	2.80×10^{-4}	4.12×10^{-4}	2.60×10^{-4}	5.64×10^{-4}	4.00×10^{-3}	1.18×10^{-3}
NS ($N\geq5$)	$0.01N^{-3}$	$0.02N^{-3}$	$0.02N^{-3}$	$0.04N^{-3}$	$0.3N^{-3}$	$0.08N^{-3}$
All NS	0.002 95	0.004 60	0.003 06	0.006 67	0.0463	0.0137
$1S \rightarrow 3D$	6.26×10^{-6}	1.67×10^{-5}	8.53×10^{-6}	2.62×10^{-5}	1.10×10^{-4}	4.90×10^{-5}
$4D$	1.30×10^{-6}	2.19×10^{-6}	1.31×10^{-6}	3.09×10^{-6}	1.98×10^{-5}	6.28×10^{-6}
ND ($N\geq5$)	$8\times10^{-5}N^{-3}$	$1\times10^{-4}N^{-3}$	$8\times10^{-5}N^{-3}$	$2\times10^{-4}N^{-3}$	$0.001N^{-3}$	$4\times10^{-4}N^{-3}$
All ND	9.5×10^{-6}	2.13×10^{-5}	1.18×10^{-5}	3.41×10^{-5}	1.54×10^{-4}	6.50×10^{-5}
Total inner-shell excitation	0.009 40	0.0262	0.0120	0.0425	0.159	0.0790
			(b) Valence-shell excitation of Li^0			
$2S \rightarrow 2P$	1.51×10^{-2}	0.367	3.89×10^{-2}	0.706	0.382	1.39
$3P$	2.40×10^{-3}	2.34×10^{-2}	5.64×10^{-3}	4.29×10^{-2}	5.74×10^{-2}	8.54×10^{-2}
$4P$	8.41×10^{-4}	7.20×10^{-3}	1.95×10^{-3}	1.31×10^{-2}	2.00×10^{-2}	2.60×10^{-2}
NP ($N\geq5$)	$0.05N^{-3}$	$0.4N^{-3}$	$0.1N^{-3}$	$0.7N^{-3}$	$1N^{-3}$	$1N^{-3}$
All NP	0.0196	0.407	0.0489	0.779	0.484	1.53
$2S \rightarrow 3S$	1.23×10^{-3}	2.39×10^{-2}	3.17×10^{-3}	4.53×10^{-2}	3.12×10^{-2}	9.02×10^{-2}
$4S$	3.88×10^{-4}	6.29×10^{-3}	9.88×10^{-4}	1.18×10^{-2}	9.77×10^{-3}	2.35×10^{-2}
$5S$	1.74×10^{-4}	2.65×10^{-3}	4.41×10^{-4}	4.96×10^{-3}	4.37×10^{-3}	9.87×10^{-3}
NS ($N\geq5$)	$0.02N^{-3}$	$0.3N^{-3}$	$0.05N^{-3}$	$0.6N^{-3}$	$0.5N^{-3}$	$1N^{-3}$
All NS	0.002 12	0.0378	0.005 42	0.0719	0.0535	0.140
$2S \rightarrow 3D$	1.89×10^{-3}	3.53×10^{-2}	4.84×10^{-3}	6.66×10^{-2}	4.78×10^{-2}	0.133
$4D$	8.46×10^{-4}	1.32×10^{-2}	2.13×10^{-3}	2.48×10^{-2}	2.11×10^{-2}	4.93×10^{-2}
ND ($N\geq5$)	$0.06N^{-3}$	$0.8N^{-3}$	$0.1N^{-3}$	$1N^{-3}$	$1N^{-3}$	$3N^{-3}$
All ND	0.004 20	0.0680	0.009 41	0.116	0.967	0.255
Total valence-shell excitation	0.0259	0.512	0.0637	0.967	0.631	1.92

TABLE II. (*Continued.*)

Li Final State (NL)	He $I_{NL,\mathrm{el}}$	He $I_{NL,\mathrm{in}}$	H_2 $I_{NL,\mathrm{el}}$	H_2 $I_{NL,\mathrm{in}}$	N $I_{NL,\mathrm{el}}$	N $I_{NL,\mathrm{in}}$
			(c) Valence-shell excitation of Li^0			
$2S \rightarrow 2P$	1.48×10^{-2}	0.373	3.81×10^{-2}	0.718	0.375	1.42
$3P$	2.83×10^{-3}	2.48×10^{-2}	5.49×10^{-3}	4.56×10^{-2}	5.55×10^{-2}	9.08×10^{-2}
$4P$	8.10×10^{-4}	7.56×10^{-3}	1.91×10^{-3}	1.38×10^{-2}	1.94×10^{-2}	2.74×10^{-2}
$5P$	3.84×10^{-4}	3.39×10^{-3}	8.97×10^{-4}	6.19×10^{-3}	9.16×10^{-3}	1.23×10^{-2}
$6P$	2.14×10^{-4}	1.83×10^{-3}	4.96×10^{-4}	3.34×10^{-3}	5.08×10^{-3}	6.61×10^{-3}
$7P$	1.31×10^{-4}	1.11×10^{-3}	3.04×10^{-4}	2.02×10^{-3}	3.12×10^{-3}	4.00×10^{-3}
NP ($N\geq8$)	$0.045N^{-3}$	$0.38N^{-3}$	$0.10N^{-3}$	$0.66N^{-3}$	$1.0N^{-3}$	$1.3N^{-3}$
All NP	0.0195	0.414	0.0481	0.795	0.476	1.57
$2S \rightarrow 3S$	1.14×10^{-3}	2.35×10^{-2}	2.96×10^{-3}	4.46×10^{-2}	2.90×10^{-2}	8.88×10^{-2}
$4S$	3.62×10^{-4}	6.22×10^{-3}	9.29×10^{-4}	1.17×10^{-2}	9.17×10^{-3}	2.33×10^{-2}
$5S$	1.63×10^{-4}	2.61×10^{-3}	4.16×10^{-4}	4.90×10^{-3}	4.11×10^{-3}	9.77×10^{-3}
NS ($N\geq6$)	$0.019\ N^{-3}$	$0.29N^{-3}$	$0.048N^{-3}$	$0.54N^{-3}$	$0.50N^{-3}$	$1.1N^{-3}$
All NS	0.001 97	0.0371	0.005 09	0.0701	0.0501	0.140
$2S \rightarrow 3D$	2.00×10^{-3}	3.84×10^{-2}	5.14×10^{-3}	7.25×10^{-2}	5.06×10^{-2}	0.144
$4D$	8.82×10^{-4}	1.41×10^{-2}	2.23×10^{-3}	2.64×10^{-2}	2.21×10^{-2}	5.26×10^{-2}
$5D$	4.54×10^{-4}	6.72×10^{-3}	1.14×10^{-3}	1.26×10^{-2}	1.13×10^{-2}	2.50×10^{-2}
ND ($N\geq6$)	$0.057N^{-3}$	$0.81N^{-3}$	$0.14N^{-3}$	$1.5N^{-3}$	$1.4N^{-3}$	$3.0N^{-3}$
All ND	0.004 27	0.0725	0.0108	0.136	0.107	0.271
Li^0 total valence-shell excitation	0.0261	0.530	0.0650	1.01	0.643	2.00
Li^0 total inelastic (HF)	0.887	1.89	0.847	2.99	12.3	6.40
Li^0 total inelastic (CI)	0.874[a]	1.86[a]	0.834	2.96	12.2[a]	6.30[a]

[a]From Ref. 19.

ample, the rapidity with which the N^{-3} extrapolation is approached. In addition, calculations have been carried out for F and G final states up through $N=5$ and for selected other higher-N states. These are not included explicitly in the Table in order to limit the table size, but they have been included in the total valence-shell excitation collision strength in Table II(c). For comparison, total inelastic collision strengths which include continuum final states as well as discrete excitations are given at the bottom of the table. Results are included for both the Hartree-Fock (HF) Li^0 ground state of Kim and Cheng[11] and for a ground state which includes configuration interactions (CI).[8]

It is beyond the scope of this work to discuss all of the systematic features of the data summarized in Table II, but a few conclusions are important for this work and should be mentioned. In terms of the relative importance for obtaining the total excitation collision strength, the $2S\rightarrow2P$ transition is clearly dominant, contributing over 50% in all cases. This is not unexpected, particularly after examining the transition strengths in Fig. 1. It should be noted that the relative contribution of this transition to the total valence-shell excitation collision strength is given *roughly* by the percentage contribution to $S_{2S\rightarrow NL}(K)$ near its maximum value (63% at $a_0K\sim\frac{1}{2}$) rather than by its contribution in the dipole limit ($M^2_{2S\rightarrow2P}/M^2_{2S\rightarrow NL}=0.99$). This simply reflects the result that the dominant region of momentum transfer in atom-atom collisions is at finite values of K, whereas electron-atom (at high energies) and photon-atom collisions are dominated by the $K\rightarrow0$ limit.

For the valence-shell transitions it is interesting to note that the dominant collision strengths occur for inelastic scattering of the target, i.e., $I_{NL,\mathrm{in}}>I_{NL,\mathrm{el}}$. For collisions among light atoms, it is generally expected that doubly inelastic collisions will be dominant over singly inelastic collisions.[19] However, the magnitude of the difference between $I_{NL,\mathrm{in}}$ and $I_{NL,\mathrm{el}}$ is quite large in these cases and, as

TABLE III. Collision strengths for the excitation and total inelastic scattering of Li^+ and Li^{2+} in high-speed collisions with He, H_2, and N. Li^+ results are based on the generalized oscillator strengths of Kim and Inokuti (Ref. 13), and the atomic form factors and incoherent scattering functions of Hubbel *et al.* (ref. 8) for He, Liu and Smith (Ref. 17) for H_2, and Tanaka and Sasaki (Ref. 18) for N. Also included are Li^+ total inelastic collision strengths from Ref. 20. The results for Li^{2+} include total excitation and total inelastic collision strengths and are computed as described in Ref. 7.

Li^+ Final State (NL)	He $I_{NL,\mathrm{el}}$	He $I_{NL,\mathrm{in}}$	H_2 $I_{NL,\mathrm{el}}$	H_2 $I_{NL,\mathrm{in}}$	N $I_{NL,\mathrm{el}}$	N $I_{NL,\mathrm{in}}$
$1S\rightarrow 2P$	1.71×10^{-2}	5.67×10^{-2}	2.39×10^{-2}	9.34×10^{-2}	0.302	0.171
$3P$	4.97×10^{-3}	1.47×10^{-2}	6.59×10^{-3}	2.38×10^{-2}	8.53×10^{-2}	4.40×10^{-2}
$1S\rightarrow 2S$	6.79×10^{-3}	1.04×10^{-2}	6.47×10^{-3}	1.44×10^{-2}	9.84×10^{-2}	2.97×10^{-2}
$3S$	1.78×10^{-3}	2.53×10^{-3}	1.62×10^{-3}	3.42×10^{-3}	2.51×10^{-2}	7.21×10^{-3}
$1S\rightarrow 3D$	2.59×10^{-4}	6.67×10^{-4}	3.65×10^{-4}	1.01×10^{-3}	4.93×10^{-3}	1.93×10^{-3}
$N(S,P,D)$ $N\geq 4$	$0.19N^{-3}$	$0.46N^{-3}$	$0.23N^{-3}$	$0.71N^{-3}$	$3.1N^{-3}$	$1.4N^{-3}$
Li^+ total excitation	0.0385	0.103	0.0482	0.164	0.639	0.310
Li^+ total inelastic	0.447[a]	0.534[a]	0.348[a]	0.720[a]	5.50[a]	1.57[a]
Li^{2+} total excitation	0.0403[b]	0.0830[b]	0.0435	0.126	0.616[b]	0.244[b]
Li^{2+} total inelastic	0.207[b]	0.234[b]	0.157	0.309	2.53[b]	0.687[b]

[a]From Ref. 20
[b]From Ref. 7

will be discussed further in Sec. IV, has significant implications for the excitation cross section of Li^0 at high speeds.

For the inner-shell excitations, the doubly inelastic collision strengths ($I_{NL,\mathrm{in}}$) are somewhat larger than the singly inelastic collision strengths ($I_{NL,\mathrm{el}}$) for He and H_2 targets, but the situation is reversed for N targets. This result is qualitatively similar to that for discrete excitations of Li^+, as might be anticipated. Table III gives a summary of comparable results for excitations to the $N=2$ and 3 levels for Li^+ colliding with He, H_2, and N. Note that while there are obvious similarities between the Li^+ and inner-shell Li^0 excitation collision strengths as regards the relative importance of particular transitions, the Li^+ NS and NP collision strengths are factors of 2—5 larger than those for Li^0. This is consistent with Eq. (10) and the magnitude of the difference is about what would be expected based on the relative magnitudes of the maximum values of the corresponding transition strengths.

For comparison, Table III also includes the total inelastic collision strengths for Li^+ from Ref. 20 for these same targets, and total excitation and total inelastic collision strengths for Li^{2+}, calculated as described in Ref. 7. Note that the total excitation collision strengths for Li^{2+} are quite close to those for Li^+, all within 25%, as would be expected from the similarities in $S_{\mathrm{ex}}(K)$ for these two ions shown in Fig. 2. The right-most inequality in Eq. (10) also assures that $I_{\mathrm{ex,el}}$ and $I_{\mathrm{ex,in}}$ for Li^+ will always be less than twice the values for Li^{2+}; hence for no target would the total excitation collision strength for Li^{2+} ever drop to below 50% of that for Li^+.

TABLE IV. Asymptotic collision strengths for electron transitions to the continuum $I_{NS\rightarrow C,\mathrm{el}}$, for fast lithium atoms and ions colliding with $Z\leq 11$ atoms, in which the target atom remains in its initial (ground) state following the collision.

		H	He	Li	Be	B	C	N	O	F	Ne	Na	
Li^0	$(2S\rightarrow C)$	0.241	0.405	1.64	3.07	4.37	5.30	6.02	6.54	6.95	7.28	9.68	$I_{2S\rightarrow C,\mathrm{el}}$
Li^0	$(1S\rightarrow C)$	0.204	0.459	1.17	2.20	3.40	4.57	5.70	6.73	7.68	8.54	10.1	$I_{1S\rightarrow C,\mathrm{el}}$
Li^+	$(1S\rightarrow C)$	0.171	0.409	0.969	1.80	2.80	3.86	4.89	5.87	6.80	7.66	9.00	$I_{\mathrm{ion,el}}$
Li^{2+}	$(1S\rightarrow C)$	0.0637	0.167	0.367	0.667	1.05	1.47	1.92	2.36	2.79	3.20	3.73	$I_{\mathrm{ion,el}}$
		1	2	3	4	5	6	7	8	9	10	11	

TABLE V. Asymptotic collision strengths for electron transitions to the continuum $I_{NS\to C,\text{in}}$ for fast lithium atoms and ions colliding with $Z \leq 11$ atoms, in which the target atom is left in an excited (discrete or continuum) state following the collision.

		H	He	Li	Be	B	C	N	O	F	Ne	Na	
Li^0	$(2S\to C)$	0.734	0.831	1.84	2.27	2.50	2.52	2.74	2.69	2.63	2.54	3.41	$I_{2S\to C,\text{in}}$
Li^0	$(1S\to C)$	0.399	0.545	0.995	1.23	1.43	1.54	1.71	1.77	1.82	1.83	2.20	$I_{1S\to C,\text{in}}$
Li^+	$(1S\to C)$	0.298	0.401	0.736	0.923	1.09	1.19	1.34	1.41	1.46	1.49	1.72	$I_{\text{ion,in}}$
Li^{2+}	$(1S\to C)$	0.0969	0.151	0.240	0.304	0.364	0.409	0.462	0.497	0.525	0.544	0.611	$I_{\text{ion,in}}$
		1	2	3	4	5	6	7	8	9	10	11	

B. Continuum final states

Asymptotic collision strengths for transitions to the continuum have also been calculated using the transition strengths $S_{1S\to C}(K)$ and $S_{2S\to C}(K)$ for Li^0 displayed in Fig. 1(c), and using $S_{\text{ion}}(K)$ for Li^+ and $Li^{2+}(K)$ shown in Fig. 2. In addition to He, H_2, and N targets, calculations have also been carried out for other atomic targets with $Z \leq 11$. The results for these calculations are summarized in Tables IV and V, corresponding respectively to the elastic or inelastic scattering of the target atom. The results in these tables utilize the atomic form factors and incoherent scattering functions given by Hubbell *et al.*[8] for all the target atoms except H (for which the analytic forms have been used[7]).

It is of interest to examine the total ionization collision strengths, given by the sum of the target elastic and inelastic contributions from Tables IV and V, as a function of the target atomic numbers. These are plotted in Fig. 3 and are referred to there as total electron-stripping collision strengths, since at high speeds these would give the electron-stripping cross sections which are important in many applications. One can readily see that the K-shell ionization collision strengths follow the general ordering expected from Eq. (9). To a fair approximation one has

$$I_{1S\to C}^{Li^0} \simeq (1.2\pm 0.1) I_{1S\to C}^{Li^+} \tag{16}$$

and

$$I_{1S\to C}^{Li^+} \simeq (2.7\pm 0.25) I_{1S\to C}^{Li^{2+}} . \tag{17}$$

The deviations from straight lines in these K-shell collision strength plots are a reflection of the shell structure of the targets, and one can discern an increasing amount of such deviation as one goes from Li^{2+} to Li^+ to Li^0. This change in sensitivity to the shell structure of the target arises primarily from the doubly inelastic contributions $I_{1S\to C,\text{in}}$

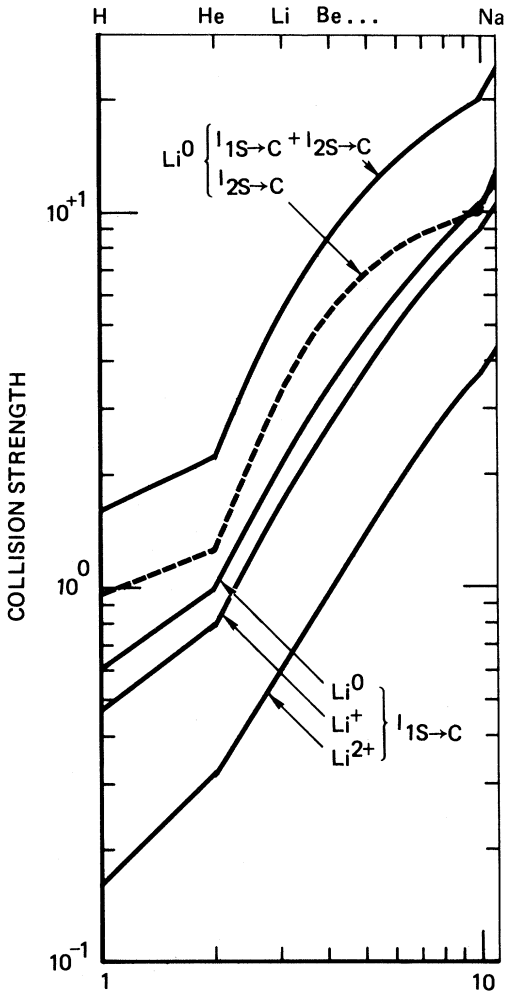

FIG. 3. Asymptotic (high-energy) collision strengths for electron stripping from lithium atoms and ions colliding with low-Z target atoms. For each projectile both the target elastic and inelastic collision strengths are added together (from Tables IV and V). For Li^0, the inner-shell ($I_{1S\to C}$) and valence-shell ($I_{2S\to C}$, dashed curve) collision strengths are shown separately as well as their sum. This sum should be a good approximation to the total ionization collision strength for Li^0, neglecting only inner-shell excitation to autoionizing states (See Table II(a) or VI for this contribution in the case of H_2, He, and N targets.)

TABLE VI. Comparison of asymptotic collision strengths for the ionization of atomic lithium calculated from two independent models of Li^0. The first results utilize Hartree-Fock wave functions for discrete Li^0 states (Ref. 11), the total valence-shell excitation collision strength is subtracted from the total inelastic collision strength to obtain the total ionization collision strength. The second case utilizes Herman-Skillman wave functions for both discrete and continuum final states (Refs. 9 and 12); results for both inner- and valence-shell transitions to both discrete and continuum final states are given. The total ionization collision strength is given by the sum of inner- and valence-shell ionization contributions plus the discrete inner-shell excitation collision strength. The percentage difference from the Hartree-Fock model with sum rules, for the total ionization and valence-shell excitation collision strengths, are indicated in parentheses. Separate results are given for the elastic and inelastic scattering of the targets. The target elastic form factors and incoherent scattering functions for these calculations are from Hubbell *et al.* (Ref. 8) for He and N, and from Liu and Smith (Ref. 17) for H_2.

	He		H_2		N	
Li atomic model Collision process	$I_{NL,\mathrm{el}}$	$I_{NL,\mathrm{in}}$	$I_{NL,\mathrm{el}}$	$I_{NL,\mathrm{in}}$	$I_{NL,\mathrm{el}}$	$I_{NL,\mathrm{in}}$
Hartree-Fock with sum rule						
Total inelastic	0.887	1.89	0.847	2.99	12.3	6.40
Valence-shell excitation	0.0261	0.530	0.0650	1.01	0.643	2.00
Total ionization	0.861	1.36	0.782	1.98	11.7	4.40
Herman-Skillman						
Inner-shell excitation	0.009 40	0.0262	0.0120	0.0425	0.160	0.0882
Valence-shell excitation	0.0259 (−0.8%)	0.513 (−3.2%)	0.0637 (−2.0%)	0.967 (−4.3%)	0.631 (−1.9%)	1.92 (−4.0%)
Inner-shell ionization	0.459	0.545	0.358	0.732	5.70	1.71
Valence-shell ionization	0.405	0.831	0.429	1.28	6.02	2.74
Total ionization	0.873 (+1.4%)	1.40 (+2.9%)	0.799 (+2.2%)	2.05 (+3.5%)	11.9 (+1.7%)	4.54 (+3.2%)

(Table V), and result in the coefficients of Eqs. (16) and (17) not being quite constants.

The L-shell ionization collision strength for Li^0 (dashed curve in Fig. 3) shows a more pronounced variation with the target atomic number than any of the K-shell results. Because the L-shell electron is much more loosely bound, and all the corresponding wave functions more diffuse than those for the K shell, the interaction with target atoms is more influenced by the longer-range parts of the potentials. Equivalently one can say that the dipole interaction regime (low K) is relatively more important for L-shell ionization than K-shell ionization. This is to be expected; what Fig. 3 gives is a quantitative summary of how these differences are reflected in collisions with neutral atoms at high speeds. Note that for Ne the different sensitivities to the target shell structure result in $I_{1S\to C}$ being larger than $I_{2S\to C}$ but the reverse applies for the remainder of the targets considered ($Z \leq 11$). Both K- and L-shell contributions to the total ionization *asymptotic* collision strength for Li^0 are important for all targets; but as will be discussed in more detail in Sec. IV, the nonasymptotic corrections to these two contributions to the cross sections are important in different energy regimes.

To conclude this section, Table VI provides a comparison of the asymptotic ionization collision strengths for Li^0 colliding with He, H_2, and N, as computed from two independent atomic models of Li^0. The first set of results is based on the Hartree-Fock transition strengths obtained from the calculations of Kim and Cheng.[11] The total valence-shell excitation collision strengths [from Table II(c)] are subtracted from the total inelastic collision strengths computed for the Hartree-Fock Li^0 ground state. The second set of results summarizes the inner-shell and valence-shell excitation and ionization collision strengths as computed for the Herman-Skillman results of McGuire.[9,12] The total asymptotic ionization collision strength is then given by the sum of the inner- and valence-shell ionization contributions together with the inner-shell discrete-excitation collisions strengths. This latter leads primarily to ionization via autodetachment rather than radiative decay back to discrete Li^0 states. Note, however, that inner-shell excitation only contributes $1-2\%$ to the total ionization collision strength in each case. For these targets, the differences in the total ionization collision strengths never exceed about $3\frac{1}{2}\%$ for these two models. Similarly the valence-shell excitation collision strengths never differ by as much as $4\frac{1}{2}\%$. These differences are the same magnitude as the expected accuracy of the numerical integrals required to obtain $S_{\rm ion}(K)$ [Eqs. (6) and (7)] and then $I_{\rm ion,el}$ and $I_{\rm ion,in}$ [Eqs. (3) and (4)]. Consequently, it is not possible to definitely assign this difference to the difference between the Hartree-Fock and Herman-Skillman atomic models, although the signs of the differences are consistent with what one might expect. If a more elaborate model of the Li^0 wave functions were utilized, which included configuration interactions for example one could expect that these asymptotic collision strengths might be reduced somewhat. However, the very small differences in the total inelastic collision strengths given in the last line of Table II(c), $0.8-1.6\%$, suggest that no significant changes in any of the major collision strengths is possible.

IV. CROSS SECTIONS AND COMPARISONS WITH EXPERIMENTAL DATA

In addition to the asymptotic collision strengths described in Section III, the second-order collision strengths, γ terms in Eq. (1), have also been calcu-

TABLE VII. Second-order collision strengths for select excitation and ionization processes of Li^0, Li^+, and Li^{2+} colliding with He, H_2, and N. These terms, together with the asymptotic collision strengths from Tables II–VI, permit the evaluation of the Born cross sections for these collision processes to two orders in an expansion in v^{-2} via Eq. (1).

Li transition	He $\gamma_{NL,\rm el}$	He $\gamma_{NL,\rm in}$	H_2 $\gamma_{NL,\rm el}$	H_2 $\gamma_{NL,\rm in}$	N $\gamma_{NL,\rm el}$	N $\gamma_{NL,\rm in}$
Li^0 $2S\to 2P$	0	−5.84	0	−2.63	0	−96.9
$2S\to NL$ (all NL)	0	−5.91	0	−2.66	0	−98.0
$S\to C$	−0.500	−0.650	−0.250	−0.571	−6.13	−5.50
$1S\to NL$ (all NL)	0	−0.196	0	−0.202	0	−1.29
$1S\to C$	−1.00	−3.64	−0.500	−5.53	−12.3	−17.1
Li^+ $1S\to C$	−1.00	−2.90	−0.500	−4.50	−12.3	−12.8
Li^{2+} $1S-C$	−0.500	−0.994	−0.250	−1.34	−6.13	−4.76

lated for several cases of interest. These terms provide an approximate way of incorporating some nonasymptotic energy dependence into the cross sections for excitation and ionization, although still within the context of the Born-approximation neglecting exchange. Formulas for these second-order collision strengths have been given in previous work.[7] They only require various energy moments of the dipole-oscillator-strength distributions such as are given in Table I for the lithium projectiles of this work and in Ref. 15 for the various target atoms. Since the computations are straightforward (algebraic), they will not be described here. For completeness Table VII gives results for the values of γ which are utilized in the cross sections for H_2, He, and N targets and which will now be discussed in some detail.

Figure 4 displays results for the theoretical K-shell ionization cross sections of Li^0 (dashed curves) and Li^+ (solid curves) in collisions with (a) He and (b) H_2. For comparison, experimental results[21–24] for the electron-stripping cross sections for Li^+ colliding with these targets are also shown. In each case, theoretical cross sections are shown for target elastic ($\sigma_{1S\to C,\mathrm{el}}$) and inelastic processes ($\sigma_{1S\to C,\mathrm{in}}$), as well as the total K-shell ionization cross section (σ_{ion}) given by the sum of these. These curves are plotted for energies above that corresponding to the maximum cross section predicted by the two-term expansion. The second-order contribution reduces the asymptotic cross section by 50% at that energy; the expansion is no longer a good approximation to the Born cross section at lower energies. These theoretical curves reflect the general result that the cross sections for the collisional ionization of the K-shell of Li^0 are modestly [Eq. (16)] larger than those for the ionization of Li^+. Note that inner-shell excitation of Li^0 has not been included.

The experimental data for electron stripping from Li^+ display some inconsistencies, as noted previously.[20] The recent experiments of Shah *et al.*[24] for H_2 appear to resolve the discrepancy between the earlier measurements of Allison *et al.*[21] and Pivovar *et al.*[22] in favor of the later values. The highest-energy data from that work[22] is also consistent with the Born calculations (σ_{ion}) of this work, although still higher-energy data are required to quantitatively test the theoretical cross sections. For He targets, the various measurements[21–23] are fairly consistent ($\sim$50%) if the earlier data of Dmitriev *et al.*[23] are corrected for metastables in the beam. However, the theoretical results of this work and the data of Pivovar *et al.* indicate that their suggested corrections lead to ground-state Li^+ stripping cross sections at 85 and 330 keV/u which appear to be too low. Their highest-energy data (750 keV/u), for which no significant metastable correction is indicated, as well as the highest-energy data of Pivovar *et al.* are in good agreement with the theoretical calculations of this work for the total Li^+ stripping cross section (σ_{ion}).

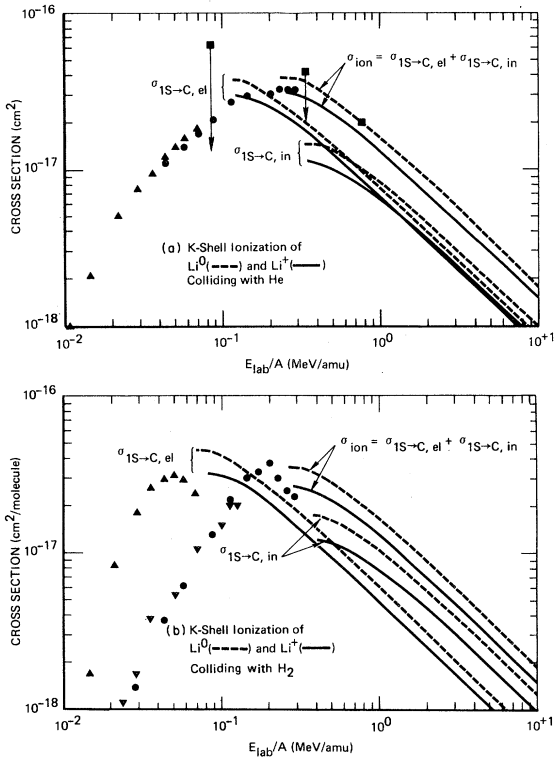

FIG. 4. Cross sections for the K-shell ionization of Li^0 and Li^+ colliding with (a) He and (b) H_2. Solid curves are the theoretical results of this work for electron stripping from Li^+, the dashed curves are those for the loss of an inner-shell electron from Li^0. In each case, results are given for the contributions arising from collisions in which the target remains in its initial state following the collision ($\sigma_{1S\to C,\mathrm{el}}$), and for collisions in which the target is either excited or ionized in the final state ($\sigma_{1S\to C,\mathrm{in}}$). Solid symbols are experimental data for electron-stripping cross sections for Li^+ from Allison *et al.* (▲, Ref. 21), Pivovar *et al.* (●, Ref. 22), Dmitriev *et al.* (■, Ref. 23), and Shah *et al.* (▼, Ref. 24). Arrows on the data of Dmitriev *et al.* indicate their suggested correction for the metastable component of their data.

For the case of neutral lithium projectiles there are significantly more inelastic processes possible associated with the presence of two electronic shells. Figure 5 summarizes the principal excitation and ionization cross sections computed in this work for

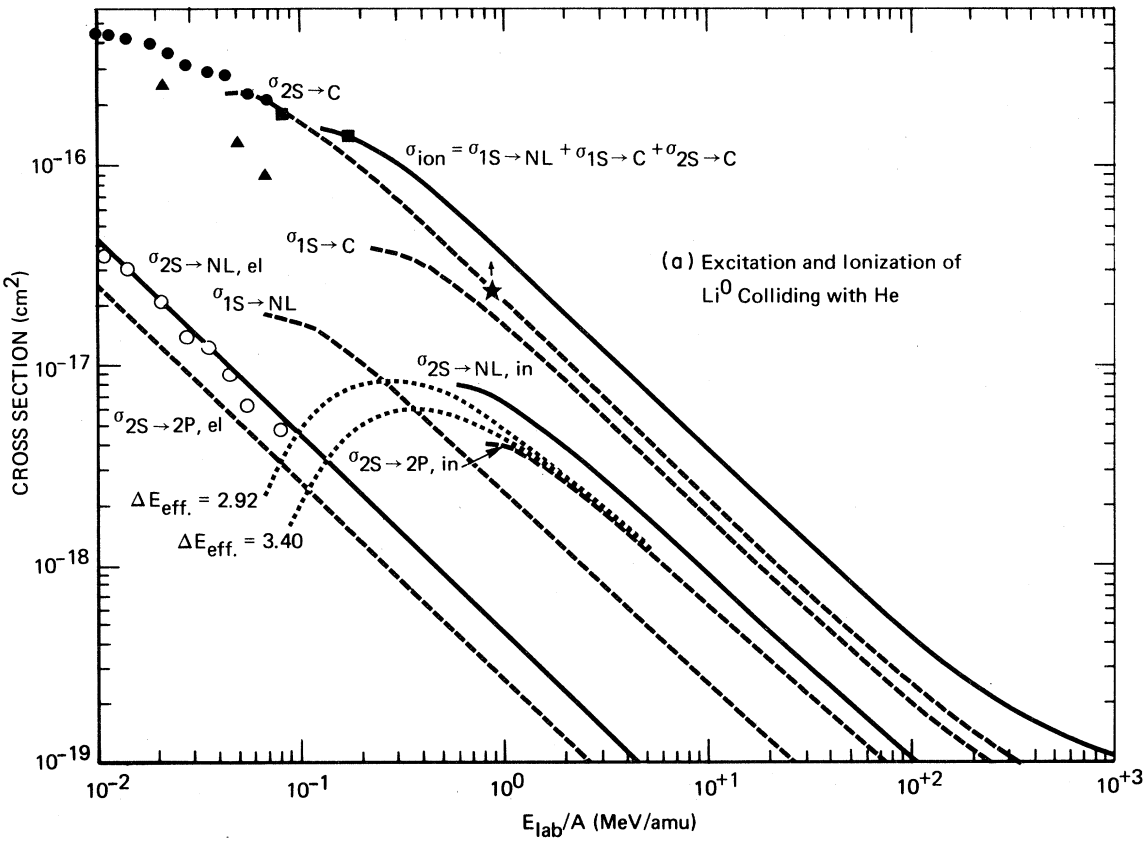

FIG. 5. Excitation and ionization cross sections for fast neutral lithium atoms colliding with (a) He and (b) H_2. Valence-shell excitation cross sections to the $2P$ final state ($2S\to 2P$, dashed curves) and to all possible discrete final states ($2S\to NL$, solid curves) are separated into the components arising from target elastic and inelastic processes. Note that target elastic scattering dominates these excitation cross sections below 50—100 keV/u, but that target inelastic collisions are the more important above 0.5—1 MeV/u. Dotted curves show the results for different approximations for $\sigma_{2S\to 2P,\mathrm{in}}$ in the intermediate energy region. Total cross sections for the ionization of lithium (σ_{ion}, solid curves) are given, as well as the separate contributions arising from valence-shell stripping ($\sigma_{2S\to C}$), inner-shell stripping ($\sigma_{1S\to C}$), and inner-shell excitation ($\sigma_{1S\to N}$) which leads to ionization via Auger emission. Solid symbols are experimental data for ionization from Allison *et al.* (▲, Ref. 21), Dmitriev *et al.* (■, Ref. 23), Horsdal-Pedersen and Hvelplund (●, Ref. 25), and Aldridge and King (✱, Ref. 5). The open symbols are experimental data for the Li^0 $2P$-$2S$ total emission cross section from Horsdal-Pedersen (○, Ref. 26).

(a) He and (b) H_2 targets, together with the available experimental data for the ionization[5,21,23,25] and $2P$-$2S$ emission[26,27] cross sections.

The valence-shell excitation cross sections have been separated according to target elastic and inelastic processes. Two excitation cross sections are shown in each case, the direct excitations to the $2P$ final state ($2S\to 2P$) and the total valence-shell excitation cross section ($2N\to NL$, solid curves). This latter cross section should be very close to the cross section for $2P$-$2S$ emissions since most of the excited states for $N\geq 3$ cascade through the $2P$ state. The branching ratios given by Nielsen *et al.*[27] together with the asymptotic collision strengths in Table II(c) have been used to estimate that 91(±7)% of $\sigma_{2S\to NL,\mathrm{el}}$ and 94(±4)% of $\sigma_{2S\to NL,\mathrm{in}}$, for both He and H_2 targets, will in fact lead to $2P$-$2S$ emission if all excited states were to decay radiatively.

There is an important difference between the theoretical excitation cross sections corresponding to target elastic and inelastic final states, namely, that the former has no low-energy correction of order v^{-4} in the expansion of the Born cross section. The doubly inelastic cross sections $\sigma_{2S\to 2P,\mathrm{in}}$ and $\sigma_{2S\to NL,\mathrm{in}}$, while over an order-of-magnitude larger than $\sigma_{2S\to 2P,\mathrm{el}}$ and $\sigma_{2S\to NL,\mathrm{el}}$ for $E/A\gtrsim 500$ keV, have sizable corrections to the asymptotic values at energies below that. The two-term theoretical cross sections for these doubly inelastic processes are only plotted for energies above that corresponding to the

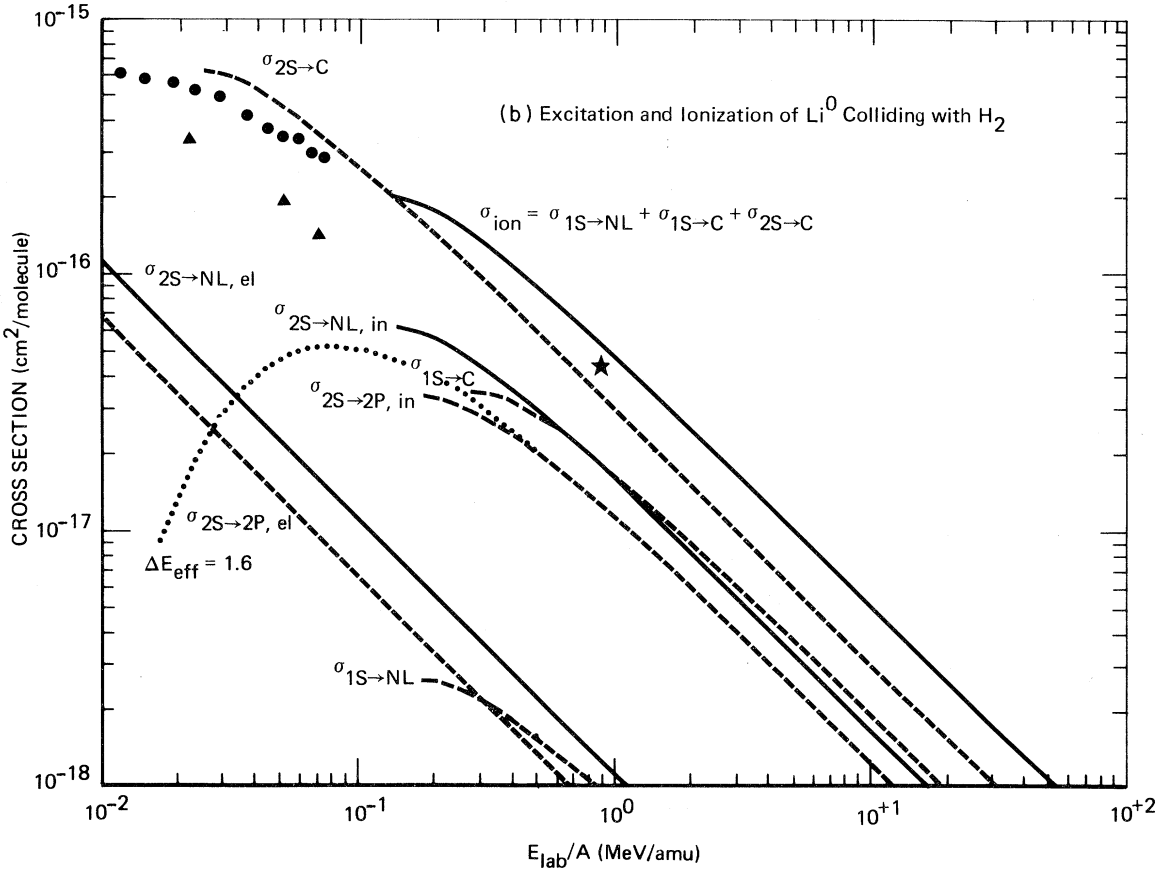

FIG. 5. (*Continued.*)

maximum value of the cross section for the same reasons as discussed in connection with Fig. 4. In order to estimate these Born cross sections at lower energies, $\sigma_{2S\to 2P,\text{in}}$ has also been computed utilizing an effective excitation energy ΔE_{eff}. This approach approximates the lower limit on momentum transfer for the collision strength integral by employing a constant value of excitation energy, independent of the particular final state. Specifically, the minimum value of momentum transfer [see Eqs. (17) and (18) of Ref. 7] is given by

$$(a_0K_{\min})^2=2\left[\frac{M}{m_e}\right]^2\frac{v^2}{v_0^2}[1-\tfrac{1}{2}x-(1-x)^{1/2}]$$
$$\simeq\tfrac{1}{4}\left[\frac{M}{m_e}\right]^2\frac{v^2}{v_0^2}x^2 \qquad (18)$$

for small x, where

$$x=\frac{(E_n+E_m)}{\frac{1}{2}Mv^2}\,. \qquad (19)$$

Here, M is the reduced mass of the colliding partners, m_e is the electron mass, v_0 is Bohr velocity, v is the initial projectile speed, and E_n and E_m are the excitation energies of the projectile and target final states, whose quantum numbers are represented by n and m, respectively. In this approximation the sum E_n+E_m is replaced by a constant ΔE_{eff}, and hence

$$a_0K_{\min}\simeq\tfrac{1}{2}\Delta E_{\text{eff}}\left[\frac{v_0}{v}\right], \qquad (20)$$

where ΔE_{eff} is in rydbergs. Sum rules can then be employed for the final states similar to the procedures used to evaluate the coefficients I and γ in Eq. (1). The result is a velocity-dependent collision strength

$$I(v)=\int_{a_0K_{\min}}^{\infty}S(K)\mathcal{F}(K)\frac{d(a_0K)}{(a_0K)^3} \qquad (21)$$

in analogy with Eq. (2), where the lower limit is now given by (20). (In terms of the nonrelativistic kinetic energy, the lower limit may also be expressed as $a_0K_{\min}=2.49\Delta E_{\text{eff}}(E_{\text{lab}}/A)^{-1/2}$, where

$E_{\rm lab}/A$ is in keV/u.)

The values of the collision strengths computed via Eq. (21), and hence the cross sections, are sensitive to the choice of $\Delta E_{\rm eff}$. A reasonable procedure for estimating $\Delta E_{\rm eff}$ is to require that an expansion of (21) for high speeds, together with (20), reproduce the γ terms appearing in Eq. (1). Other estimates which yield similar values for $\Delta E_{\rm eff}$ have been employed in other work,[28] but this particular procedure does not appear to have been used before. For the doubly inelastic collision strength $I_{2S\to 2P,\rm in}$, this approach gives

$$\Delta E_{\rm eff}=\left[\frac{-8\gamma_{2S\to 2P,\rm in}}{M^2_{2S\to 2P}M^2_{\rm tot}}\right]^{1/2}, \tag{22}$$

where $M^2_{2S\to 2P}$ is the dipole matrix element squared for the $2S\to 2P$ transition of lithium and $M^2_{\rm tot}$ is the total squared dipole matrix element for the target. From the dipole-oscillator-strength data of McGuire $M^2_{2S\to 2P}=5.43$. Together with the values of $M^2_{\rm tot}$ for He and H_2,[20] and the $\gamma_{2S\to 2P,\rm in}$ results from Table VII, formula (22) gives 3.4 and 1.6 rydbergs for $\Delta E_{\rm eff}$ for He and H_2, respectively. Results for the cross section $\sigma_{2S\to 2P,\rm in}$ using these values of $\Delta E_{\rm eff}$ are given by dotted curves. For the case of a He target, results for a 14% decrease in $\Delta E_{\rm eff}$ (to 2.9) are also given to display the sensitivity to this parameter.

The $2P$-$2S$ emission cross section measured by Horsdal-Pedersen[26] for a He target is in very good agreement with the values of $\sigma_{2S\to NL,\rm el}$ calculated in this work. This theoretical cross section is also in good agreement with the $2P$-$2S$ emission cross section measurements of Nielsen *et al.*[27] [not shown in Fig. 5(a)] for energies down to about 2 keV/u.[29] Furthermore their basic interpretation of those measurements as being describable in terms of collisions in which the He is treated as a static charge distribution is consistent with these Born-approximation results indicating that doubly inelastic collisions are not important below about 100 keV/u. However, the theoretical curves shown in Fig. 5(a) do indicate that a significant departure from a v^{-2} extrapolation of these low-energy data can be expected somewhere in the 100–500-keV/u energy region. Above 1 MeV/u or so, a v^{-2} scaling is again expected, but with a coefficient roughly 20 times that appropriate to low energies. For H_2 targets [Fig. 5(b)], the theoretical results of this work are qualitatively similar to those for a He target, except that this transition region between singly inelastic and doubly inelastic dominated collisions is at lower energies: 20–100 keV/u.

These results for two different regimes for Li^0 collisional excitation are also qualitatively similar to those for H^0 collisional $1S\to 2P$ excitation.[7,28,30] However, two differences between the Li^0 and H^0 excitation calculations should be noted. The magnitude of the difference between the doubly and singly inelastic asymptotic cross section is larger for $2S\to 2P$ excitation of Li^0 than it is for the $1S\to 2P$ excitation of H^0. More importantly, the valence-shell excitations of Li^0 correspond to significantly lower excitation energies than for H^0 excitation from the ground state. This means that the Li-He collisions are dominated by lower momentum transfer than the case of H-He collisions. Hence, the Born approximation should be more reliable in predicting these cross sections at the lower energies, a conclusion supported by the limited data available at present.

The cross sections leading to electron loss from the Li^0 $\sigma_{\rm ion}$ in Fig. 5 have been divided into the components arising from the different electronic shells. The inner-shell excitation cross sections ($\sigma_{1S\to NL}$) have also been included in $\sigma_{\rm ion}$ but they are a relatively small contributor. The dominant contributions arise from direct collisional ionization from both shells, each contributing nearly equally to $\sigma_{\rm ion}$ at high energies. This result was also obtained by Dewangan and Walter using a free collision model to describe electron loss.[31] The effective values for their asymptotic collision strengths for K-shell and L-shell ionization have been estimated from Fig. 9 of their paper for He and Ne (and Ar) targets and, with one exception, are well within 10% of the values obtained in this work. The one exception is the K-shell ionization collision strength for a He target, where their effective value of $I_{1S\to C,\rm el}+I_{1S\to C,\rm in}$ appears to be about 25% lower than that given by Tables IV and V here. Consequently, they concluded that for the case of a He target about 37% of the asymptotic cross section for electron loss from Li^0 arose from K-shell ionization—the results obtained here indicate a contribution of nearly 45%. This is, overall, a relatively minor discrepancy and the close agreement with the free collision model attests to its utility when carefully applied.

An important difference in the inner- and valence-shell ionization cross sections is the different energy required to approach the asymptotic value. For beam energies below about 100 keV/u, the results of this work indicate that the observed cross sections for electron stripping are completely dominated by ionization of the valence-shell elec-

tron. The values of $\sigma_{2S\to C}$ are also in good quantitative agreement with the experimental data of Dmitriev *et al.*[23] and Horsdal-Pedersen and Hvelplund[25] for a He target; the data of Allison *et al.*[21] are inconsistent with both these other experiments and the theoretical results. For H_2, the theoretical curve for $\sigma_{2S\to C}$ is about 20% above the Horsdal-Pedersen and Hvelplund data,[25] and again the data from Ref. 21 are significantly lower. Data at higher energies are clearly sparse. The highest energy data of Dmitriev *et al.* for a He target are consistent with the theoretical results, but the combined uncertainty of the experimental data and the theoretical $\sigma_{1S\to C}$ contribution to σ_{ion} in the 100–200-keV/u transition region is sizable. The recent data of Aldridge and King[5] at 6/7 MeV/u are somewhat below the theoretical curve for σ_{ion}, but would be consistent with the $\sigma_{2S\to C}$ contribution alone. There are some ambiguities in the extraction of these cross sections from the raw charge-state data which do not permit a definitive conclusion to be drawn. For example, the arrow on the He data indicates how that cross section would be changed if the ratio $\sigma_{0,1}/\sigma_{-1,0}$ had been determined from the maximum observed neutral yield rather than from the target density at the position of that maximum. No significant correction of this type occurs for H_2, but the anomalous behavior of the raw charge-state data for that gas raises other questions.

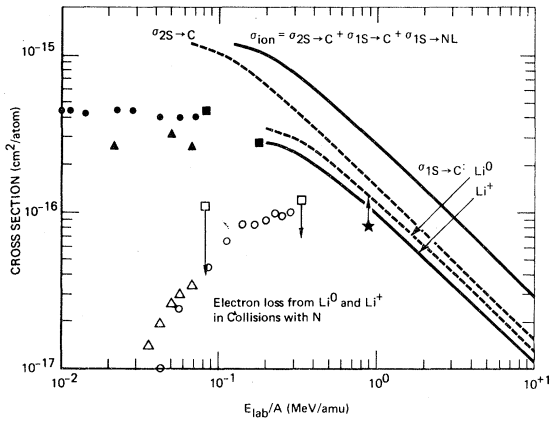

FIG. 6. Cross sections for electron loss from fast Li^0 and Li^+ colliding with nitrogen. Solid curves give the theoretical results of this work for the total ionization cross section for Li^0 (σ_{ion}) and Li^+ ($\sigma_{1S\to C}$); broken curves give the two dominant contributions to the Li^0 ionization cross section arising from the valence- and inner-shell transitions to the continuum. Solid symbols are experimental data for Li^0 electron-stripping cross sections $\sigma_{0,1}$, and open symbols are Li^+ stripping cross sections $\sigma_{1,2}$, from Allison *et al.* (△▲, Ref. 21), Dmitriev *et al.* (□■, Ref. 23), Horsdal-Pedersen and Hvelplund (●, Ref. 25), Aldridge and King (★, Ref. 5), and Pivovar *et al.* (○, Ref. 22). All experimental data are for N_2 gas and have divided by two for comparison with the atomic N calculations.

As a final application of some of the results given in this work, Fig. 6 gives a comparison of theoretical and experimental cross sections for electron loss from Li^0 and Li^+ colliding with nitrogen. Many of the theoretical results discussed in relation to H_2 and He targets are relevant to other targets and need not be reiterated. A primary difference for the heavier targets is the higher energy required before the Born approximation is applicable. This is evident in Fig. 6 where the available Li^0 and Li^+ data are significantly below the calculated cross sections. Even with the possible correction (of the type discussed for He) to the data of Aldridge and King, their results for $\sigma_{0,1}$ at 6/7 MeV/u would still be less than $\frac{1}{2}$ of the theoretical results for σ_{ion}. The magnitude of this discrepancy is somewhat surprising at first as the experimental electron-loss cross sections for H^0 in the (more tightly bound) $1S$ state are only about 35% below similar theoretical results at this speed, and the electron-loss cross sections for H^0 in the $2S$ state are within about 30% at even lower speeds ($\frac{1}{2}$ MeV/u).[16] It may be that while the electron-stripping cross section from the valence shell in Li-N collisions at 6/7 MeV/u has reached its asymptotic (v^{-2}) form, the inner-shell electron-loss cross section is still significantly below the theoretical Born prediction at that speed. Further experimental data on Li^0 collisions would obviously be of interest in this velocity regime.[32]

V. CONCLUDING REMARKS

A fairly comprehensive summary of theoretical results for the high-speed Born cross sections for excitation and ionization of lithium projectiles colliding with low-Z atomic and molecular H_2 targets has been presented. The theoretical uncertainty in the *asymptotic* collision strengths presented, and hence in the high-energy cross sections, is generally no more than about 5%. This uncertainty is associated with both the accuracy of numerical integrations and the difference between different atomic models of the Li transition strengths. Results for Li^+ and Li^{2+} are correspondingly more accurate, while inner-shell Li^0 excitation cross sections (small in magnitude) may be less accurate.

While these asymptotic cross sections are expected to be quite accurate, the energy at which experimental results should begin to follow the asymptotic Born predictions depends very critically on the inelastic process under consideration. This energy can be as low as 2 keV/u for the $2P$-$2S$ Li^0 emission cross sections in collisions with light targets (H_2,He) to a few 100 keV/u for K-shell electron loss in the same targets, and perhaps several MeV/u for the heavier targets (still with $Z \leq 11$). The importance of the different energy regimes for different processes is dramatically displayed in the case of $2P$-$2S$ emission cross sections, where the v^{-2} trend of the experimental data for 2—100 keV/u (He targets) is expected to change by more than an order-of-magnitude above 1 MeV/u, due to the increased importance of doubly inelastic processes. Similarly, most of the available experimental data for Li^0 electron loss probably corresponds to valence-shell stripping, while inner-shell ionization is expected to be equally important at higher energies. It is hoped that these theoretical predictions will prompt further experimental work on this simplest multishell atom.

ACKNOWLEDGMENTS

The author is indebted to Jack Aldridge for useful discussions on the details of the Li^- stripping experiment described in Ref. 5, and to Erik Horsdal-Pedersen for providing his $2P$-$2S$ emission cross sections prior to publication. The assistance of Ralph Janda in carrying out some of the numerical work is greatly appreciated. This effort was supported by the Defense Advanced Research Projects Agency under Contract No. DASG60-C-81-0023.

[1]Alec N. Broers, Phys. Today 32, No. 11, 39 (1979); R. L. Seliger, J. W. Ward, V. Wang, and R. L. Kubena, Appl. Phys. Lett. 34, 310 (1979).

[2]C. L. Olson, J. Fusion Energy 1, 309 (1982); D. Keefe, Annu. Rev. Nucl. Part. Sci. 32, 391 (1982).

[3]L. R. Grisham, D. E. Post, D. R. Mikkelsen, and H. P. Eubank, Nucl. Technol.—Fusion 2, 199 (1982).

[4]L. R. Grisham, D. E. Post, B. M. Johnson, K. W. Jones, J. Barette, T. H. Kruse, I. Tserruya, and W. Da-Hai, Rev. Sci. Instrum. 53, 281 (1982).

[5]J. P. Aldridge and J. D. King, Los Alamos Scientific Laboratory Report No. LA-8682-MS (unpublished).

[6]R. W. McCullough, M. B. Shah, M. Lennon, and H. B Gilbody, J. Phys. B 15, 791 (1982).

[7]G. H. Gillespie, Phys. Rev. A 18, 1967 (1978).

[8]J. H. Hubbell, Wm. J. Veigele, E. A. Briggs, R. T. Brown, D. T. Cromer, and R. J. Howerton, J. Phys. Chem. Ref. Data 4, 471 (1975); 6, 615 (1977).

[9]E. J. McGuire, Sandia Laboratories Report No. SC-RR-70-406, pp. 13—17 (unpublished); see also Ref. 12.

[10]F. Herman and S. Skillman, *Atomic Structure Calculations* (Prentice-Hall, Englewood Cliffs, N.J., 1963).

[11]Y.-K. Kim and K.-t. Cheng (private communications).

[12]For momentum transfer in the interval $0.0961 \leq (a_0K)^2 \leq 0.66$, the $2S \rightarrow 2P$ generalized oscillator strengths for Li tabulated in Ref. 9 are not correct, being 30—50% too low. The $2S \rightarrow 2P$ transition strength shown in Fig. 1(b), and the other calculations in this work, utilize newly computed values for this generalized oscillator strength [E.J. McGuire (private communications)].

[13]Y.-K. Kim and M. Inokuti, Phys. Rev. A 12, 102 (1975); tabulated data for the Li^+ generalized oscillator strengths were kindly provided by Y.-K. Kim (private communication).

[14]Y.-K. Kim, Argonne National Laboratory Report No. ANL-7615, 209 (unpublished).

[15]J. L. Dehmer, M. Inokuti, and R. P. Saxon, Phys. Rev. A 12, 102 (1975); M. Inokuti, T. Baer and J. L. Dehmer, *ibid.* 17, 1229 (1978); select partial moments for these works kindly provided by M. Inokuti (private communication).

[16]G. H. Gillespie, Phys. Rev. A 22, 454 (1980).

[17]J. W. Liu, Phys. Rev. A 7, 103 (1973); J. W. Liu and V. H. Smith, J. Phys. B 6, L275 (1975).

[18]K. Tanaka and F. Sasaki, Int. J. Quantum Chem. 5, 157 (1971).

[19]G. H. Gillespie and M. Inokuti, Phys. Rev. A 22, 2430 (1980).

[20]G. H. Gillespie, Y.-K. Kim, and K.-t. Cheng, Phys. Rev. A 17, 1284 (1978).

[21]S. K. Allison, J. Cuevas, and M. Garcia-Munoz, Phys. Rev. 120, 1266 (1960).

[22]L. I. Pivovar, Yu. A. Levchenko, and G. A. Krivonsov, Zh. Eksp. Teor. Fiz. 59, 19 (1970) [Sov. Phys.—JETP 32, 11 (1971)].

[23]I. S. Dmitriev, V. S. Nikolaev, Yu. A. Tashaev, and Ya. A. Teplova, Zh. Eksp. Teor. Fiz. 67, 2047 (1974) [Sov. Phys.—JETP 40, 1017 (1975)]; I. S. Dmitriev, V. S. Nikolaev, L. N. Fateeva, and Ya. A. Teplova, *ibid.* 42, 16 (1962) [*ibid.* 15, 11 (1962)].

[24]M. B. Shah, T. V. Goffe, and H. B. Gilbody, J. Phys. B 11, L233 (1978).

[25]E. Horsdal-Pedersen and P. Hvelplund, J. Phys. B 6, 1277 (1973).

[26]E. Horsdal-Pedersen, preliminary results (private communication).

[27]S. E. Nielsen, N. Andersen, T. Andersen, J. O. Olsen, and J. S. Dahler, J. Phys. B 11, 3187 (1978).

[28]H. Levy, Phys. Rev. 185, 7 (1969).

[29]The $\sigma_{2S\to 2P,\mathrm{el}}$ cross section for a He target has also been calculated at lower energies during the course of this work using essentially the exact Born cross section; specifically by using $\Delta E_{\mathrm{eff}}=E_{2S\to 2P}=0.135$ Ry in Eqs. (20) and (21). This cross section is reduced from the asymptotic Born results by only 10% at 1.2 keV/u.

[30]R. H. Hughes and S.-S. Choe, Phys. Rev. A 5, 656 (1972).

[31]D. P. Dewangan and H. R. J. Walters, J. Phys. B 11, 3983 (1978).

[32]One additional experimental result for $\sigma_{0,1}$ in Li-O_2 collisions at 6/7 MeV/u is available in Ref. 5. The asymptotic theoretical results of this work (Tables IV and V) give a cross section of 3.6×10^{-16} cm^2/at; the low-energy corrections (analogous to those in Table VII) reduce this by about 8%. The experimental value for $\sigma_{0,1}$ from Ref. 5 is nearly 60% below this; furthermore, possible corrections of the type indicated in Figs. 5(a) and 6 *reduce* the cross section in this case so that it is more than 75% below the theoretical results.